International Journal of Advanced Technology and Engineering Exploration, Vol 9(93)
ISSN (Print): 2394-5443 ISSN (Online): 2394-7454
http://dx.doi.org/10.19101/IJATEE.2021.875728

Research Article

Experimental and numerical study of forced convictive heat transfer in a horizontal circular pipe with varying angles ribs

Sarmad A. Abdul Hussein[1*] and Suhaib J. Shbailat[2]
Department of Mechanical Engineering, College of Engineering, University of Baghdad, Baghdad, Iraq[1]
Department of Biomedical Engineering, Al-Esraa University College, Baghdad, Iraq[2]

Received: 02-April-2022; Revised: 19-August-2022; Accepted: 21-August-2022

Abstract
The forced convective of heat transfer in the horizontal circular pipe without and with using the different angles of circular ribs (60°, 90° and 120°) were studied experimentally and numerically. The circular pipe was made from stainless steel of 500 mm length and 49 mm inner diameter. The circular ribs of 20 mm diameter were arranged one against the other with a distance of 100 mm between one rib and another. Air was used as a working fluid. The effect of varying Reynolds numbers (12557 to 17954) with constant surface pipe temperature of 325 K on enhancing convective heat transfer without and with using circular ribs were investigated. The experimental side included manufacturing the test section and conducting a series of experiments to show effect of varying the Reynold numbers on energy transfer and air flow characteristics. Numerical simulation included using ANSYS FLUENT (18.2) program to solve the governing equations with using Simple algorithm method and Standard k–ε turbulence model. The comparisons between the experimental results and the numerical simulation results were carried out. In general, results showed that average coefficient of the heat transfer and average Nusselt number with ribs angle of 60° were the largest compared to the other ribs angle and smooth circular pipe. The heat transfer coefficient was increased with increasing Reynolds numbers. The circular horizontal pipe with ribs angle of 60° gives a good evidence for the performance of thermal- hydraulic applications.

Keywords
Forced convection, ANSYS FLUENT, Turbulent flow, Circular ribs, Gas turbine.

1.Introduction
Heat transfer is one of the most important processes that can have very large applications in human life. It can range from conversion, exploitation, and utilization of recovered thermal energy in large industrial applications, domestic and commercial applications. In large industrial applications, it is important to add and subtract the heat with the high efficiency. There are several methods of heat transfer; one of the most important is forced convection heat transfer. Among the common applications in our daily life is heat transfer in pharmacy, the process of condensing steam in electric power plants as well as its use in agricultural products. The goal of all these applications is to increase the process of heat transfer by forced convection [1].

The improvement of heat transfer is essential to enhance the performance of various heat transfer systems. Improving the thermal performance of devices such as solar fluids heaters and heat exchangers used in many industrial applications leads to savings in thermal energy and materials used.

The above systems and their performance are relvent to the power and energy industry [2−5], thermal management [6−8], packaging of electronics and electronic components [9−11], aerospace technologies [12, 13], and engines [14, 15], and new construction techniques [16, 17]. The researchers using various methods to enhance the heat transfer processes, including the addition of materials to the liquid-like nanomaterial [18−21], wire mesh coils and twisted tapes insertion [22−24], and the use of corrugated finned and spirally corrugated tubes [25, 26]. People have turned their attention to the sun in an effort to find alternative sources of viable energy. On the other hand, the thermal performance of the

*Author for correspondence

solar heater is poor due to the low rate of heat transfer from the absorption plate to the working fluid. It has been suggested that the sun might be a possible source of alternative energy in an endeavor to develop alternative sources of viable energy. Due to the low rate of heat transfer from the absorption plate to the working fluid, the thermal performance of a solar heater is suboptimal [27].

Many methods that employed to enhance the heat transfer rate by convection, especially in the engine of gas turbine lanes used to cool the turbine blades. These methods uses fins, ribs, baffles, jet impact cooling, drooping surfaces, roughness of the surface, burr surfaces and the other types of the turbulence triggers. All the methods aim to increase the characteristics of fluid flow, heat transfer coefficient and significantly reduce pressure losses. From these data, the appropriate design for such tasks is determined. Ribs on the duct walls have been used to enhance the rates of heat transfer in ducts. Roughness from the presence of continuous or gapped ribs has the ability to break up the boundary layer at the heat transfer surface, and this causes a reduction in thermal resistance while also boosting heat transferred by causing turbulence in a laminar flow. When dealing with turbulent flow, the ribs can enhance the turbulence intensity even more, and this causes to increase the coefficient of heat transfer even more. Furthermore, the rate of heat transfer is raised as a result of the larger heat transfer area created by the mounted ribs, which increases the rate of heat transmission [28]. Furthermore, the rate of heat transfer is raised as a result of the larger heat transfer area created by the mounted ribs, which increases the rate of heat transmission [28].

The rest of the paper is organized as follows. Literature review was discussed in section 2. Section 3 covers the method. Results and discussion were investigated in section 4. Conclusion is in section 5.

2.Literature review

In order to improve heat transfer in these applications, a diversity of techniques based on focused on active and passive concepts have been suggested. This paper reviewed the roughness geometry used in the heat transfer applications and reported the roughness optimum geometry that was adapted. Rambhad et al. [29] mathematically and experimentally examined the heat transfer and fluid flow parameters in a circular pipe inserting vortex flow generator to improve the thermal performance of forced convective heat transfer. Aljibory et al. [30] investigated numerically and experimentally the characteristics of fluid flow and heat transfer in a circular pipe with various rib constructions at constant temperature and with varying Reynolds numbers. Pandey et al. [31] studied numerically the heat transfer and fluid flow characteristics in a circular tube using Y- shape baffles. Kore et al. [32] conducted an experimental investigation on the properties of fluid flow and heat transfer in a rectangular duct employing three distinct forms of ribs; the square, house and boot shapes. The mechanisms of forced convective heat transfer in a circular pipe inserting of the twin coil was presented by Dang and Wang [33]. Rasool et al. [34] studied the effects of a binary chemical reaction, thermal radiation, and Soret- Dufour effects on the incompressible static flow of Darcy-Forchheimer nanofluids. Chanmak et al. [35] investigated experimentally the forced convective heat transfer characteristics in a circular pipe using porous wire mesh. Fadhil et al. [36] studied experimentally and numerically effect of the using semicircular ribs on two fluids flow (air and water) and the coefficient of heat transfer in the rectangular channel with varying of heat flux and velocities of the water and air. Al et al. [37] investigated experimentally and numerically the influence of the pitch spacing of the rib in a turbulent ribbed tube on the fluid flow rate and coefficient of the heat transfer. Golam [38] examined the rib forms effect on the characteristics of convective heat transfer in a square passage, and his findings were supported by experimental evidence. Round, triangular, and square ribs were among the rib shapes that were employed. It was investigated by Choi et al. [39] that utilizing a rib- dimpled channel, they could explore numerically the features of heat transfer and fluid flow. At constant Reynolds number, the effect of rib angle variation and the distance between the center of the rib and the rim of the dimple were investigated in detail. Nakhchi and Esfahani [40] conducted a numerical investigation into the increase of convective heat transfer in a circular pipe utilizing several rib shapes, including flat conical, right angle, and variations in the height, width, and pitch of the rib. Sadiq and Hamza [41] looked the effect of distance between the ribs on heat transfer inside a rectangular duct with constant and variable heat flow, as well as with and without Nano fluids. Wang et al. [42] examined numerically the enhancement of heat transfer in circular pipe using trapezoid ribs and smooth pipe at constant Reynolds number. Theeb and Mussa [43] conducted a numerical investigation of the effect of combining cross ribs with diagonal ribs on the fluid flow rate

and the heat transfer and characteristics of rectangular duct with a large proportion of incoming air. When the cross ribs were utilized, the rate of heat transfer was found to be increased, according to the findings of the study. Dhaidan and Abbas [44] investigated the numerical simulation of heat transfer enhancement and turbulence flow in corrugated pipes with varied rib shapes; rectangular ribs, semicircular ribs, and trapezoidal ribs were all investigated. Hashim [45] performed a numerical analysis of the effects of using fan-shaped ribs as a motor in a rectangular duct on the behaviors of heat transfer and pressure drop. Alwan et al. [46] studied numerically and experimentally the effect of Nano fluids flow with inserting of twisted tape on the heat transfer and fluid flow characteristics in a circular pipe. The effect of combining cross ribs with diagonal ribs on the fluid flow rate and the heat transfer and characteristics of rectangular duct with a large proportion of incoming air were presented by Alfarawi et al. [47]. Hammoodi et al. [48] investigated numerically the effect of inserting three types of ribs on the heat transfer performance and fluid flow characteristics.

The present work presents an experimental and numerical case study of forced convective heat transfer inside a horizontal circular pipe with varying circular ribs angles to compare with smooth circular pipe. the numerical analysis using ANSYS FLUENT (18.2) program for three dimensional and steady state condition were compared to the experimental data to choose the best model to simulate the convective heat transfer and fluid flow in a horizontal circular pipe without and with varying angles circular ribs. The result provides the best ribs angle which can be selected in designing of the circular pipe as a simulation for blades of the gas turbine.

3.Methods

3.1Experimental apparatus and data reduction

The experimental apparatus that was designed and constructed to investigate forced convective heat transfer within a horizontal circular pipe with and without the use of circular ribs at a constant pipe surface temperature is depicted schematically and photographically in *Figures 1* and *2*, respectively. The test section was consisted of blower unit, air velocity controller, wood box and two electrical heaters. The horizontal circular pipe was made from stainless steel with dimensions (600 mm length and 49 mm inner diameter) that putted inside a rectangular wood box (500 mm length, 300 mm width and 300 mm high).The two electrical wire heaters (500 Watt) were installed on walls of the box. The air blower was connected directly with the test section. The air entered the horizontal circular pipe with change of the air velocity (5.5, 6, 6.5, 7 and 7.5) m/s. Five circular ribs were made from stainless steel (25 mm length and 20 mm diameter) as shown in *Figure 3*. The circular ribs were installed inside a circular pipe at different angles (60°, 90° and 120°) to select the best angle that provided a more turbulence effect to choose the suitable design of test present section. The temperatures of the rig were measured using 10 thermocouples (type K). Five thermocouples were inserted into the circular pipe center at different spacing (thermocouple for each 10 cm) to measure the air flow temperature. Three thermocouples were placed at the outer surface of the pipe and two thermocouples at the outer surface of the wood box to measure the heat loss. The calibration of thermocouples was carried out by subjecting each thermocouple to fixed point environments (distilled water boiling at 100 ^{o}C and ice point at 0 ^{o}C at atmospheric pressure). They also subject to the boiling point of acetone (56.1 ^{o}C).

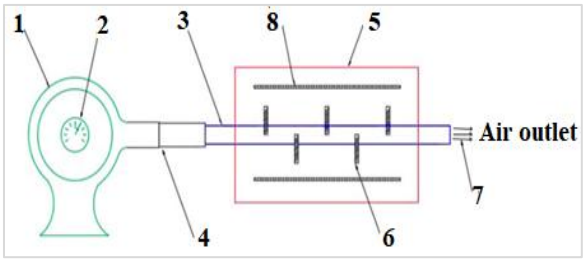

1-Blower 2- Air velocity Controller 3- Pipe 4- Nozzle
5- Wood Box 6- Ribs 7- Air outlet 8-Heater
(a) Parts of the device with ribs

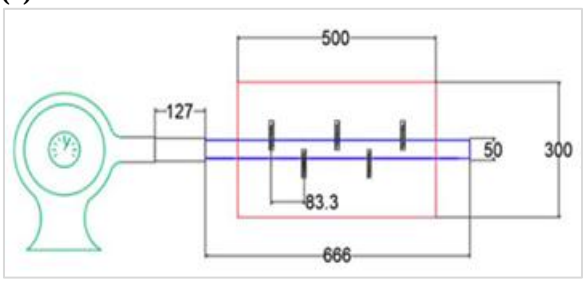

(b) Dimensions of the experimental apparatus (mm)
Figure 1 Schematic diagram of the experimental device

Representation of this line in a straight-line equation gives, Papulová et al. [49] (Equation 1);

T_{true}(K type) = 0.56 + 0.979 (1)

The air velocity controller was used to control the air velocity flow of the circular pipe. The heat loss was

recorded to about 4% during the total range of the heat transfer rate.

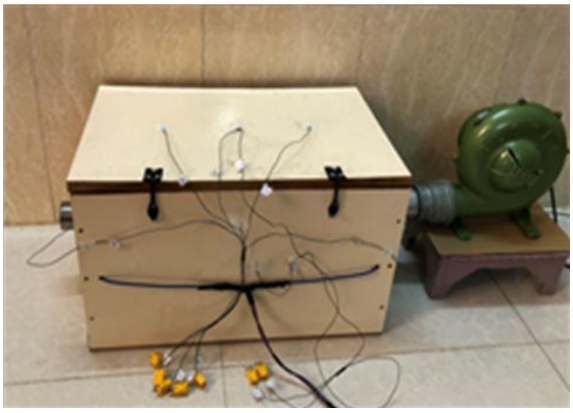

Figure 2 Photograph of the experimental apparatus

Figure 3 Photograph of installing circular ribs (90°)

3.1.1Error analysis

The experimental results accuracy can be affected by two factors ; the measurements accuracy and device designing nature. Interval of the uncertainty (w) in a result can be written by the following correlation, Delort et al. [50] (Equation 2):

$$w_R = \left[\sum_{i=1}^{n}\left(\frac{\partial R}{\partial ai}\, w_i\right)^2\right]^{1\backslash 2} \quad (2)$$

Where, R represents the result, e is an independent parameter and n is summation of independent parameters (*Table 1*).

Table 1 presents the experimental errors which may be occurred in the independent parameters e. These errors are taken from the measuring devices as shown below

Independent parameter (e)	Uncertainty (w)
Temperature	± 0.1 °C
Volume flow rate	± 0.03 m^3/s
Pipe diameter	± 0. 005 m
Pipe length	± 0. 005 m

3.1.2Data analysis

Simplified steps are employed to analyze process of the heat transfer of the air flow rate in horizontal circular pipe without ribs and with varying ribs angles (60°, 90° and 120°) which are inserted in different distances of the circular pipe under conditions of constant pipe surface temperature and varying Reynolds numbers.

To determine the air mass flow rate $\dot{m}$ inside the horizontal circular pipe by applying the Equation 3:

$$\dot{m} = \rho v A \quad (3)$$

Where ρ represents the mean air density, v is the air velocity and A is cross section area of the circular pipe. Reynolds number Re can be determined depending on the hydraulic diameter and inlet velocity of the fluid as shown in Equation 4:

$$Re = \frac{\rho v D_h}{\mu} \quad (4)$$

Where, D_h is the hydraulic diameter of a horizontal circular pipe and μ is the dynamic viscosity of the air. The convective heat transfer Q to the air can be calculated from the following Equation 5:

$$Q = \dot{m} C_p (T_{a,o} - T_{a,i}) \quad (5)$$

Where, C_p is the air specific heat, $T_{a,o}$ is outlet air temperature, and $T_{a,i}$ is temperature of the inlet air.

Coefficient of the overall heat transfer h from pipe surface to air flow inside a circular pipe can be written as shown in Equation 6:,

$$h = \frac{Q}{A_s(T_s - T_{a,m})} \quad (6)$$

Where, A_s is the surface area of circular pipe, T_s is temperature of the surface pipe and $T_{a,m}$ is a mean bulk temperature.

Nusselt number Nu can be calculated from the following Equation 7,

$$Nu = \frac{h D_h}{k} \quad (7)$$

Where, k represents the thermal conductively of the air**.**

3.2Numerical simulation

The numerical simulation was presented to study effect of the circular ribs on characteristics of the heat transfer and compare to the smooth pipe. The geometry with varying angles circular ribs can be shown in *Figure 4.* The length of the circular pipe is 500 mm and 49 mm inner diameter, the distance between ribs was 100 mm, the outer pipe surface was

kept with constant surface pipe temperature of 325 K. Three angles of circular ribs were studied with varying Reynolds numbers (12557, 13887, 15224, 16568 and 17954). ANSYS FLUENT software package (version 18.2) was simulated to solve continuity, momentum, and energy equations. The numerical analysis is presented for three-dimensional, steady state, turbulent flow and forced convection heat transfer. Air was used as an ideal gas as the working fluid. The governing equations described the air flow field in the fluid region. Continuity equation, Navier Stokes equation and energy equation can be written;

Conservation of mass equation is shown in Equation 8.

$$\frac{\partial \rho}{\partial t} + \nabla.(\rho \vec{v}) = 0 \quad (8)$$

Conservation of momentum equation is shown in Equation 9.

$$\frac{\partial (\rho \vec{v})}{\partial t} + \nabla.(\rho \vec{v}\vec{v}) = \rho g - \nabla P + \nabla.(\bar{\bar{\tau}}) \quad (9)$$

Conservation of energy equation is shown in Equation 10.

$$\frac{\partial (\rho E)}{\partial t} + \nabla.\left(\vec{v}(\rho E + p)\right) = \nabla.(k_{eff}\nabla T + (\bar{\bar{\tau}}_{eff}.\vec{v}) \quad (10)$$

Where;

$$\bar{\bar{\tau}} = \mu(\nabla \vec{v} + \nabla \vec{v}^T) - \frac{2}{3}\nabla.\vec{v}I) \quad (11)$$

$$E = h + \frac{P}{\rho} + \frac{v^2}{2} \quad (12)$$

I, in Equation 11 represents the identity matrix and μ is symbol to the dynamic viscosity.

The model of RNG k- ϵ used two equations to find the first one for specific turbulent kinetic energy equation (k) and the second for rate of the turbulent dissipation equation (ϵ) (Equation 13).

$$\frac{\partial (\rho k)}{\partial t} + \frac{\partial}{\partial x_i}(\rho k v_i) = \frac{\partial}{\partial x_i}\left(\alpha_k \mu_{eff}\frac{\partial k}{\partial x_i}\right) + G_k + G_b - \rho\varepsilon \quad (13)$$

$$\frac{\partial (\rho \varepsilon)}{\partial t} + \frac{\partial}{\partial x_i}(\rho \varepsilon v_i) = \frac{\partial}{\partial x_i}\left(\alpha_\varepsilon \mu_{eff}\frac{\partial k}{\partial x_i}\right) + C_{1\varepsilon}\frac{\varepsilon}{k}(G_k + C_{3\varepsilon}G_b) - C_{1\varepsilon}\frac{\varepsilon}{k}(G_k + C_{3\varepsilon}G_b) - C_{2\varepsilon}\rho\frac{\varepsilon^2}{k} - R_\varepsilon \quad (14)$$

Since the steady state is assumed, so the term $\frac{\partial}{\partial t}$ in the equations were neglected. All terms meanings that used in the RNG k- ϵ model were explained in the fluent documents [51].

Using the structure of the mesh and method of the finite volume to resolve incompressible 3-D Navier-Stokes equations. *Figure 5* shows the mesh that formed to model the circular pipe with and without using circular ribs. the model mesh was three dimensional with triangular meshes type. The number of nodes and elements were varied depending on the presence or absent the circular ribs. With using circular ribs was 35819 nodes and 94999 elements while in the case of smooth pipe was 31985 nodes and 91880 elements.

The boundary condition of the air inlet was included that the air inlet temperature of 300 K and the air velocities were varied in each case at (5.5, 6, 6.5, 7 and 7.5) m/s. the boundary condition of the air outlet was considered as an atmospheric pressure outlet. The boundary condition of the circular ribs was considered as wall, surface of the circular pipe at constant temperature of 325K. The solution method that used in all cases was algorithm SIMPLE for velocity – pressure coupling. Upwind schemes for momentum, turbulence kinetic energy. A hexagonal grid has been used in the present work. In case presence ribs, the calculations were carried out with and without ribs. The elements are more near the ribs and near wall element spacing close to y^+ = 8 to calculate the experimental model. Convergence will occur when the Convergence Criterion for each variable was reached. When the residuals were satisfied to 10^{-4} and 10^{-7}, then the solution was said to be converging. *Figure 6* showed that all the scaled residuals were below 10^{-4} and 10^{-7}. The parameters were considered to set the boundary conditions for the solution of the governing equations of the turbulent forced convection.

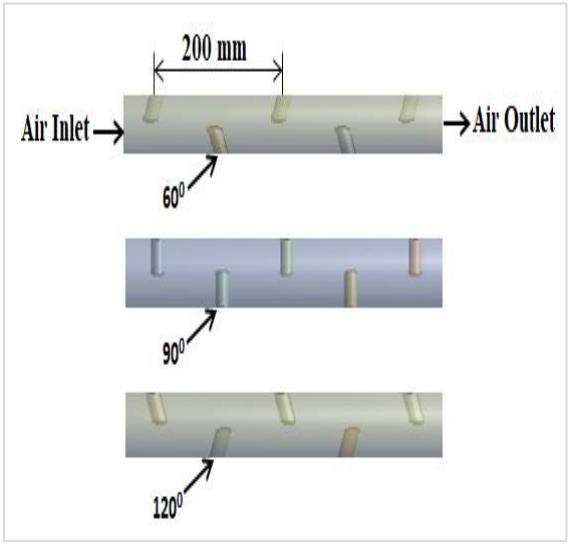

Figure 4 Test section geometry with varying angles ribs

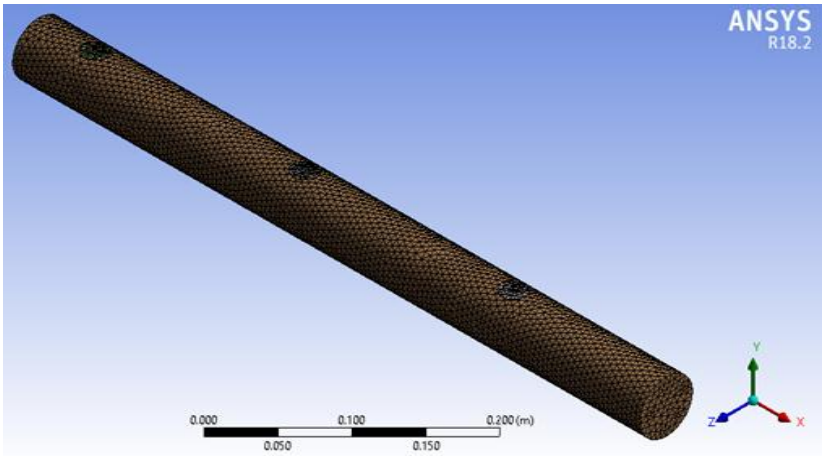

(a) Mesh generation with 60° ribs angles (3D**)**

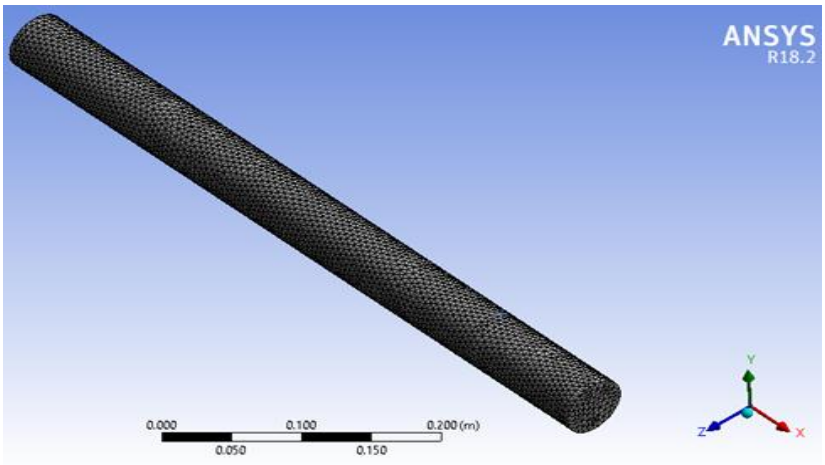

(b) Mesh generation without ribs (3D)

Figure 5 Mesh generation of the used models

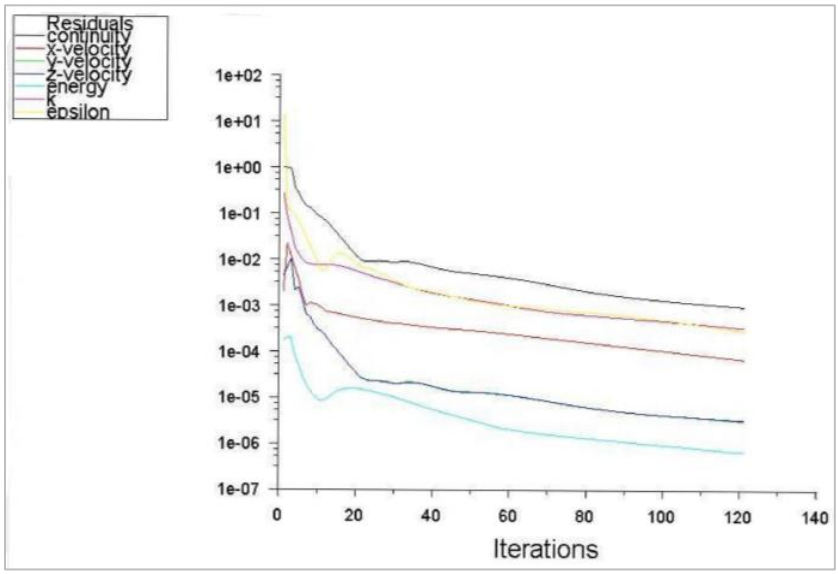

Figure 6 Convergence history to solve discrete conservation equations (Re=17954)

4.Result and discussion

4.1Analysis of numerical results

Figures 7 and *8* show the numerical results for varying Reynolds numbers in a horizontal circular pipe with different angles of the ribs. *Figure 6* shows the average outer air temperature versus Reynolds numbers with and without using ribs.

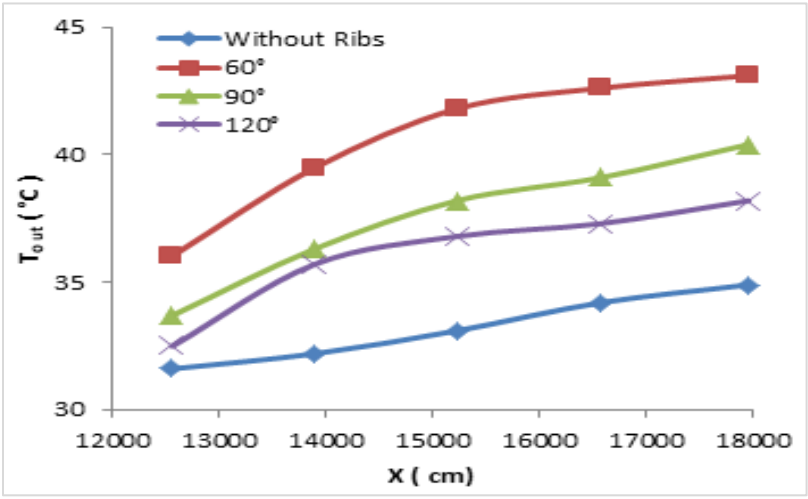

Figure 7 Average outer air temperatures with and without ribs

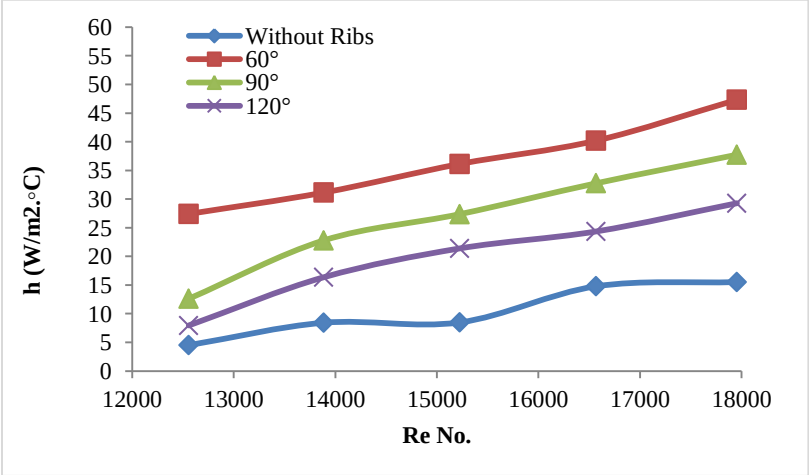

Figure 8 Average heat transfer coefficient air temperatures with and without ribs

It's noted from the figures that average outer air temperature increase with increasing Reynolds numbers. Highest of air temperatures are recorded with angle rib 60° and lowest of air temperatures are recorded without using ribs. *Figure7* shows the effect of varying Reynolds numbers on average of the heat transfer coefficient with and without using circular ribs. The result show that the average of heat transfer coefficient increases with increasing Reynolds numbers. Its recorded maximum values with the ribs at different angles and the highest values using ribs at angle 60° because the turbulent force is increased as increase of the air force resistance.

The temperature distribution contours of smooth pipe and circular ribs with varying angles ribs (60°, 90° and 120°) at outer surface pipe temperature of 325 K, temperature of air inlet of 301 K and 17954 Reynolds number are shown in *Figures 9 (a to d).* In general, it is noted from the figures that the air coolant temperature is low at the beginning of the circular pipe and gradually increases to reach the maximum possible at the end of the circular pipe due to increase of the heat stored along circular pipe. Also, it's shown that the air coolant temperature near the wall is more affected by the ribs especially at angle 60° because the ribs create a great resistance against the

passage of coolant air. Thus, the heat transfer is increased between the air flow and the hot pipe surface as a result of the increased air turbulence force.

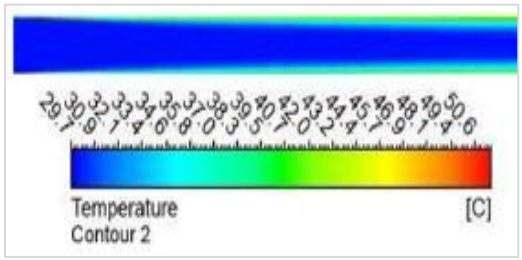

(a)Without ribs

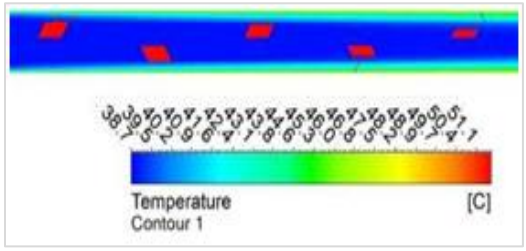

(b) 60°

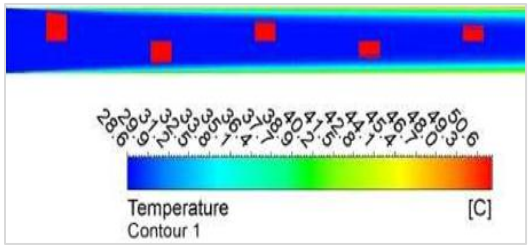

(c) 90°

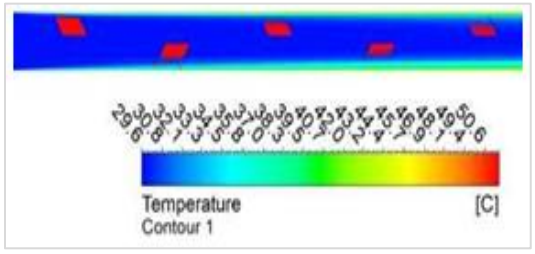

(d) 120°

Figure 9 Air temperature distribution contours with and without circular ribs

Figures 10 (a to d) present the velocity distribution contours of a smooth circular pipe and with varying angles ribs. It's shown from the *Figure 10 (a)* that the velocity of cooling air decreases at the central line of the air passage continuously throughout the pipe, while it is noted from the *Figures 10 (b to d)* that due to the contraction and expansion of the air flow over circular ribs, the air flow accelerates and slows down through the pipe passage.

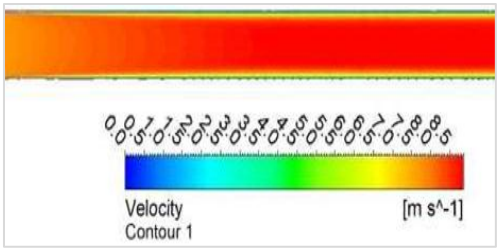

(a)Without ribs

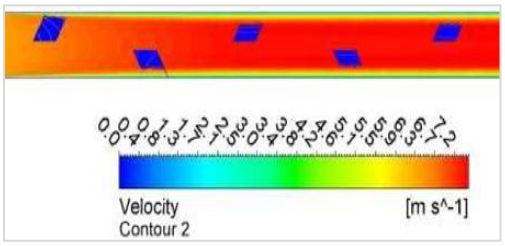

(b)60°

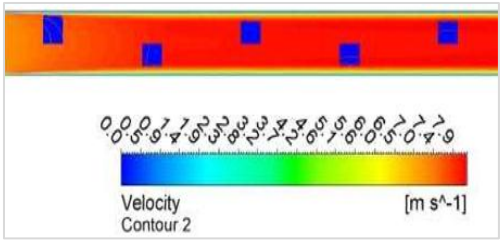

(c)90°

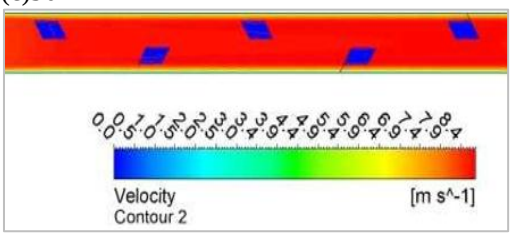

(d) 120°

Figure 10 Air velocity distribution contours with and without circular ribs

Figures 11 and *12* present a comparison between the air streamline without and with using ribs at angle 60° respectively at Reynolds number of 17954. It can be clearly seen that the stream lines in the case of using ribs are more smoothly moving towards exit section and there is no circulations in all inclination angles, while the stream lines in the case using ribs are less smoothly moving towards the exit section. And this evidence that the turbulence force with using ribs is more than of smooth pipe and this gives more enhancements in the heat transfer towards the exit section.

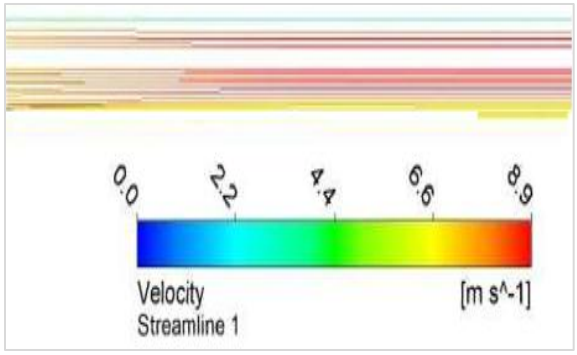

Figure 11 Velocity streamline in circular pipe without ribs

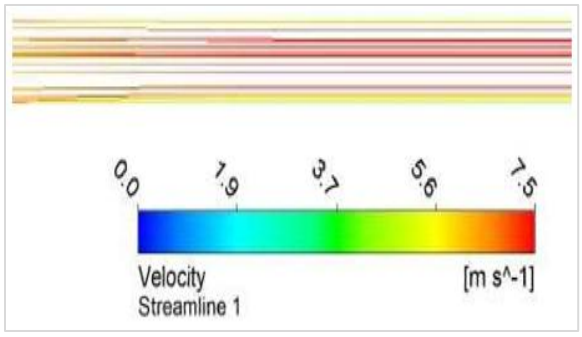

Figure 12 Velocity streamline in circular pipe with angle ribs of 60°

4.2 Analysis of experimental results

A series of experiments is performed under constant pipe surface temperature of 325 K and varying Reynolds numbers from 12557 to 17954. The temperature distribution along the horizontal circular pipe is measured. The effect of change of air temperature and Reynolds numbers on local and mean heat transfer coefficient are analyzed and discussed. The general correlations of Nusselt number average as a function of Reynold numbers is presented to consider the behavior of heat transfer and rate of fluid flow in circular pipe with and without circular ribs.

The air temperature variation in a horizontal circular pipe without and with varying angles ribs are plotted in *Figures 13* and *14*. The figures show the experimenter air temperature distribution along circular pipe at lowest and highest Reynolds number of 12557 and 17954 respectively. In general, it is noted from the figures that the air temperature increases from the pipe entrance and attains to a maximum value at end of the pipe.

The rate of surface temperature increases linearly proportional to the pipe distance.

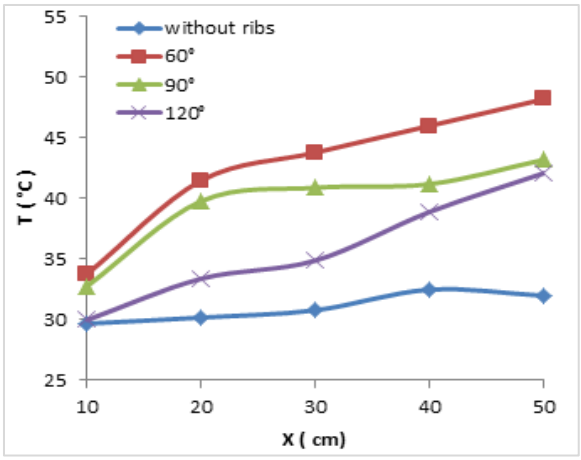

Figure 13 Air temperatures distribution along circular pipe (Re=12557)

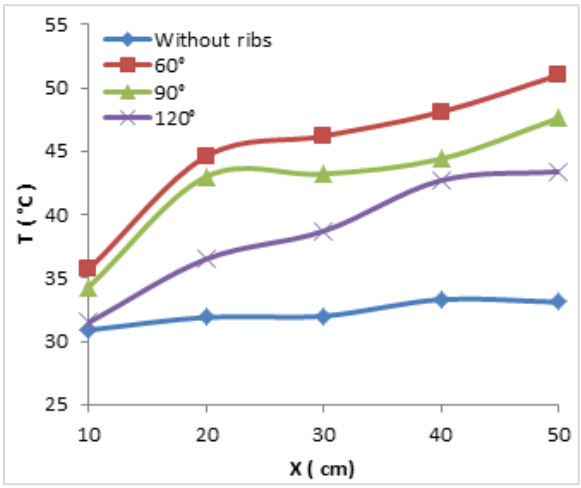

Figure 14 Air temperatures distribution along circular pipe (Re=17954)

Figure 15 shows the air temperature difference between inlet and outlet fluid temperature versus varying Reynolds number without and with varying ribs angles (60°, 90° and 120°). It's shown that the temperature difference is decreased with increasing Reynolds numbers. The maximum temperature difference is recorded at angle of 60° due to the ribs in this angle creates a high resistance versus the fluid flow causing to increase of the turbulence force inside the circular pipe.

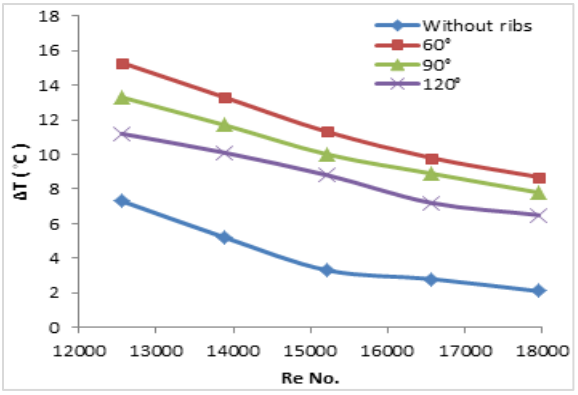

Figure 15 Air temperatures difference with and without varying angles ribs

The influence of Reynolds numbers variation on average heat transfer coefficient with varying ribs angles are presented in *Figure16*. The local heat transfer coefficient is increased with increasing Reynolds numbers to reach to a maximum value at Reynolds number of 17954 and angle ribs of 60° due to due to increasing in difference of the air temperature between surface pipes and mean of the air temperature as a result of increase of the thermal boundary layer thickness.

Figure 17 presents variation of the average Nusselt number with varying Reynolds numbers values. The figure demonstrates that increasing Reynolds numbers are raised the average of Nusselt number. In general, each process of the heat transfer with using circular ribs is appeared more effectiveness compared to smooth circular pipe because in the case of presence ribs is more transport of the heat as a result of increasing thermal boundary layer thickness that caused to increase turbulence force of fluid flow inside a circular pipe.

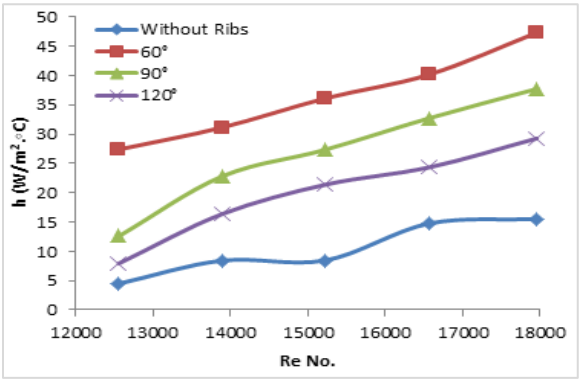

Figure 16 Average heat transfer coefficient with and without ribs

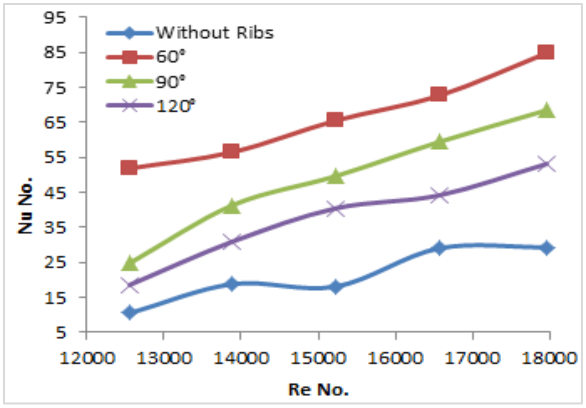

Figure 17 Average Nusselt number with and without ribs

4.3Comparison experimental and numerical results

The characteristics of heat transfer and fluid flow in horizontal circular pipe with and without using circular ribs at different angles are measured. *Figures 18* and *19* show the comparison between experimental data and numerical simulations with varying Reynolds numbers. The average outer air temperatures with smooth pipe are shown in *Figure 18*. Results of the numerical simulation give a good agreement to the experimental data. The variations of average Nusselt numbers with varying Reynolds number are shown in *Figure 19.* The figure shows a clear convergence between the numerical results and the experimental data to a large extent. It is also noted from the figure that average Nusselt number for the experimental data are less than numerical results about 12.5%.

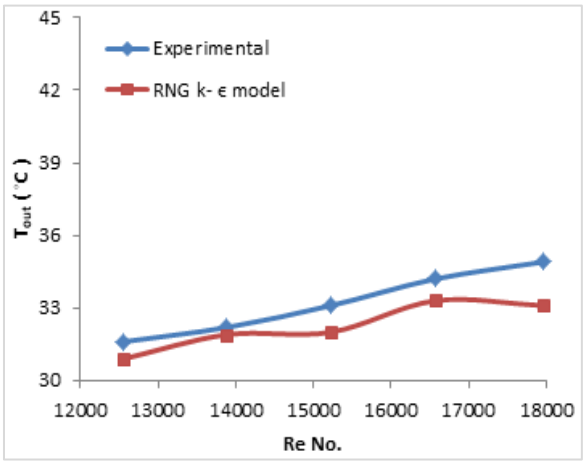

Figure 18 Average outer air temperatures without ribs

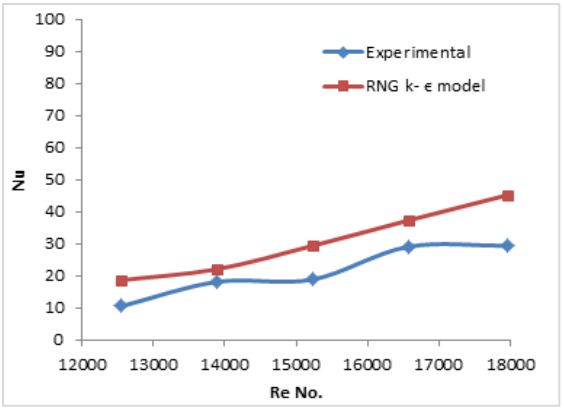

Figure 19 Average Nusselt number without ribs

Figures 20 and *21* show the comparison between experimental results and numerical simulations for different Reynolds numbers with angle ribs 60°. *Figure 20* shows the average outer air temperatures increases with increase of the Reynolds numbers. It's noted from *Figure 21* that the average Nusselt numbers increases with increasing Reynolds numbers. The deviations between the experimental data and the numerical predictions are less than 14%.

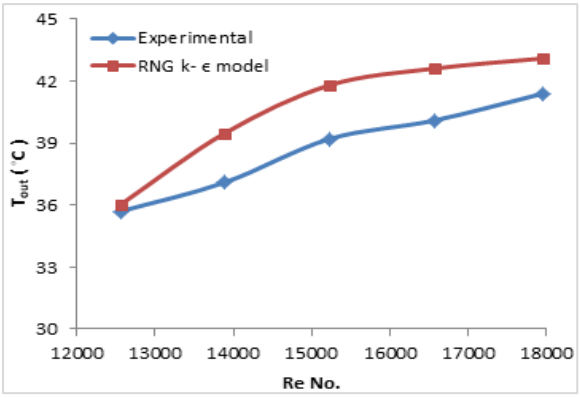

Figure 20 Average outer air temperatures with angle ribs of 60°

Local Nusselt numbers for convective heat transfer in a horizontal circular pipe are calculated with and without using circular ribs by the following correlations, Lienhard and John [52] and Wang et al. [53].

The local Nusselt number equation is shown by Equation 15.

$$\frac{Nu_x}{Nu_\infty} = 1 + 0.416Pr^{-0.4}\left(\frac{x}{d_h}\right)^{-0.25}\left(1 + \frac{3600}{Re\sqrt{\frac{x}{d_h}}}\right)\exp\left(-0.17\frac{x}{d_h}\right) \quad (15)$$

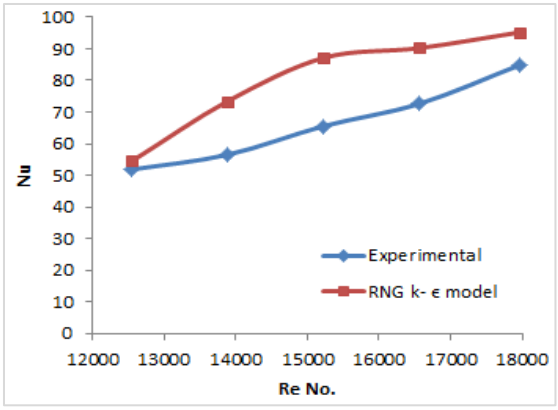

Figure 21 Average Nusselt number with angle ribs of 60°

The average Nusselt number equation is shown by Equation 16.

$$Nu_\infty = \frac{\left(\frac{\xi}{8}\right)RePr}{1+\frac{900}{Re}+12.7\sqrt{\xi/8}\left(Pr^{\frac{2}{3}}-1\right)} \quad (16)$$

For Reynold numbers;

$$(4000 \le Re \le 10^6, 0.7 \le Pr \le 100, \frac{x}{d_h} > 0.5)$$

Also, the average Nusselt number equation is shown in Equation 17.

$$Nu_\infty = \frac{\left(\frac{\xi}{8}\right)(Re-1000)Pr}{1+12.7+12.7\sqrt{\xi/8}\left(Pr^{\frac{2}{3}}-1\right)} \quad (17)$$

For Reynold numbers;

$$(2300 \le Re \le 10^4, 0.5 \le Pr \le 200)$$

Where ξ is Darcy friction factor is shown in Equation 18.

$$\xi = (1.82logRe - 1.64)^{-2} \quad (18)$$

Figures 22 and *23* compare the experimental results with the results of a numerical simulation and the local Nusselt numbers correlations in a horizontal circular pipe with and without using circular ribs for Reynolds number 17954 respectively. The figures show that the local Nusselt numbers is reduced along a circular pipe and numerical results give a good agreement with experimental results than to local Nusselt numbers correlations. The divergence between experimental results and numerical simulation are less than 8% without circular ribs, while by using circular ribs at angle 60° is given less than 12%.

A complete list of abbreviations is shown in *Appendix I.*

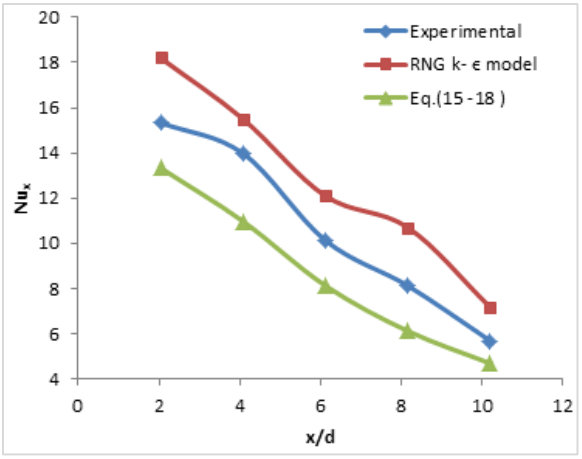

Figure 22 Local nusselt number without ribs (Re=17954)°

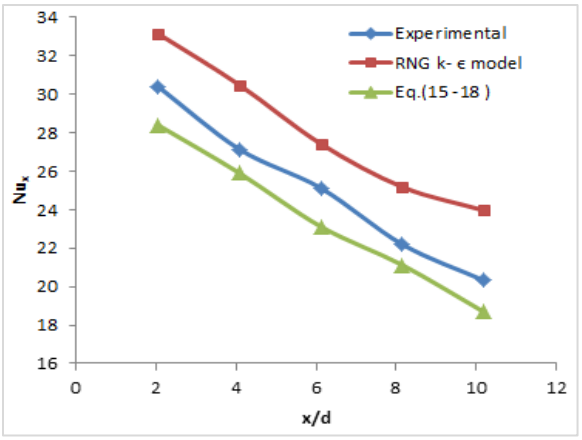

Figure 23 Local nusselt number with angle ribs of 60° (Re=17954)

5. Conclusion

The presented experimental and numerical work investigated the effect of varying angles ribs on the characteristics of heat transfer and fluid flow in horizontal circular pipe. In general, the conclusions are shown that the thermal performance of circular pipe with varying angles ribs give better results compared to the smooth pipe, especially with angle rib of 60°. The average Nusselt number for experimental results are less than of numerical results about 11.5%. The local Nusselt number for experimental results and numerical simulation are diverged about 8% without ribs, while with angle rib of 60° is given to about 12%. The behavior of the experimental and numerical results gives a good agreement compared to the local Nusselt numbers correlations. The local and average of the heat transfer coefficient increases with increase of the Reynolds numbers. The circular horizontal pipe with angle rib of 60° gives a good evidence for the performance of thermal- hydraulic applications.

Acknowledgment

None.

Conflicts of interest

The authors have no conflicts of interest to declare.

Author's contribution statement

Sarmad A. Abdul Hussein: Data collection, conceptualization, writing – original draft, analysis and interpretation of results. **Suhaib J. Shbailat:** Study conception, design, data collection, supervision, investigation on challenges and draft manuscript preparation.

References

[1] Mashkour MA, Majdi HS, Habeeb LJ. Enhancement of forced convection heat transfer in tubes and heat exchangers using passive techniques: a review. Journal of Mechanical Engineering Research and Developments. 2021; 44(3):208-18.

[2] Alva G, Lin Y, Fang G. An overview of thermal energy storage systems. Energy. 2018; 144:341-78.

[3] Wang J, Xie H, Guo Z, Cai L, Zhang K. Using organic phase-change materials for enhanced energy storage in water heaters: an experimental study. Journal of Enhanced Heat Transfer. 2019; 26(2):166-78.

[4] Omar IAA, Hammoodi KA, Ali AM. Experimental and theoretical comparison between metallic and mirror reflectors with different receiver tank. Journal of Mechanical Engineering Research and Developments. 2020; 43(7):51-61.

[5] Basem A, Moawed M, Abbood MH, El-maghlany WM. The energy and exergy analysis of a combined parabolic solar dish–steam power plant. Renewable Energy Focus. 2022; 41:55-68.

[6] Basem A, Moawed M, Abbood MH, El-maghlany WM. The design of a hybrid parabolic solar dish–steam power plant: an experimental study. Energy Reports. 2022; 8:1949-65.

[7] Terekhov VI, Khafaji HQ, Gorbachev MV. Heat and mass transfer enhancement in laminar forced convection wet channel flows with uniform wall heat flux. Journal of Enhanced Heat Transfer. 2018; 25(6):565-77.

[8] Feng L, Zhou S, Li Y, Wang Y, Zhao Q, Luo C, et al. Experimental investigation of thermal and strain management for lithium-ion battery pack in heat pipe cooling. Journal of Energy Storage. 2018; 16:84-92.

[9] Yilmazoglu MZ, Gokalp O, Biyikoglu A. Heat removal improvement in an enclosure with electronic components for air conditioning devices. Journal of Enhanced Heat Transfer. 2019; 26(1):1-14.

[10] Zhang WH, Lin WK, Yeh CT, Chiang SB, Jao CS. A novel liquid-packaging technology for highly reliable UV-LED encapsulation. Heat Transfer Research. 2019; 50(4):349-60.

[11] Guo Z. A review on heat transfer enhancement with nanofluids. Journal of Enhanced Heat Transfer. 2020; 27(1):1-70.
[12] Sapounas AA, Nikita-martzopoulou C, Martzopoulos G. Numerical and experimental study of fan and pad evaporative cooling system in a greenhouse with tomato crop. In international symposium on high technology for greenhouse system management: greensys. 2007 (pp. 987-94).
[13] Ligrani P, Mcinturff P, Suzuki M, Nakamata C. Winglet-pair target surface roughness influences on impingement jet array heat transfer. Journal of Enhanced Heat Transfer. 2019; 26(1):15-35.
[14] Kim NH. Steam condensation enhancement and fouling in titanium corrugated tubes. Journal of Enhanced Heat Transfer. 2019; 26(1):59-74.
[15] Dong F, Cao T, Hou L, Ni J. Optimization study of artificial cavities on subcooled flow boiling performance of water in a horizontal simulated engine cooling passage. Journal of Enhanced Heat Transfer. 2019; 26(1):37-57.
[16] Huang K, Deng X. Enhanced heat and mass transfer of falling liquid films in vertical tubes. Journal of Enhanced Heat Transfer. 2018; 25(1):79-96.
[17] Iasiello M, Cunsolo S, Bianco N, Chiu WK, Naso V. Fully developed convection heat transfer in open-cell foams. Journal of Enhanced Heat Transfer. 2018; 25(4-5):333-46.
[18] Mohammad WS, Murtadha TK, Ahmed KA. Using termodeck system for pre-cooling/heating to control the building inside conditions. Al-Khwarizmi Engineering Journal. 2014; 10(3):13-24.
[19] Sathish T. Performance improvement of base fluid heat transfer medium using nano fluid particles. Journal of New Materials for Electrochemical Systems. 2020; 23(4):235-43.
[20] Wang J, Hashemi SS, Alahgholi S, Mehri M, Safarzadeh M, Alimoradi A. Analysis of exergy and energy in shell and helically coiled finned tube heat exchangers and design optimization. International Journal of Refrigeration. 2018; 94:11-23.
[21] Maithani R, Kumar A, Sharma S. Effect of straight slot rib height on heat transfer enhancement of nanofluid flow through rectangular channel. Materials Today: Proceedings. 2022; 50:1159-63.
[22] Manjunath K. Heat and fluid flow behaviors in a laminar tube flow with circular protruded twisted tape inserts. Case Studies in Thermal Engineering. 2022.
[23] Ravikiran B, Ramji K, Subrahmanyam T. Investigation on thermal performance of different wire coil twisted tape inserts in a tube circulated with water. International Communications in Heat and Mass Transfer. 2021.
[24] Singh SK, Sarkar J. Hydrothermal performance comparison of modified twisted tapes and wire coils in tubular heat exchanger using hybrid nanofluid. International Journal of Thermal Sciences. 2021.
[25] Safarzadeh S, Niknam-azodi M, Aldaghi A, Taheri A, Passandideh-fard M, Mohammadi M. Energy and entropy generation analyses of a nanofluid-based helically coiled pipe under a constant magnetic field using smooth and micro-fin pipes: experimental study and prediction via ANFIS model. International Communications in Heat and Mass Transfer. 2021.
[26] Xie JH, Cui HC, Liu ZC, Liu W. Optimization design of helical micro fin tubes based on exergy destruction minimization principle. Applied Thermal Engineering. 2022.
[27] Duffie JA, Beckman WA. Solar engineering of thermal processes. John Wiley & Sons; 2013.
[28] Peng H, Ding G, Hu H. Effect of surfactant additives on nucleate pool boiling heat transfer of refrigerant-based nanofluid. Experimental Thermal and Fluid Science. 2011; 35(6):960-70.
[29] Rambhad KS, Kalbande VP, Kumbhalkar MA, Khond VW, Jibhakate RA. Heat transfer and fluid flow analysis for turbulent flow in circular pipe with vortex generator. SN Applied Sciences. 2021; 3(7):1-21.
[30] Aljibory MW, Rashid FL, Alais SM. An experimental and numerical investigation of heat transfer enhancement using annular ribs in a tube. In IOP conference series: materials science and engineering 2018 (pp. 1-20). IOP Publishing.
[31] Pandey L, Prajapati H, Singh S. CFD study for enhancement of heat transfer and flow characteristics of circular tube heat exchanger using Y-shaped insert. Materials Today: Proceedings. 2021; 46:9827-36.
[32] Kore SS, Dingare SV, Chinchanikar S, Hujare P, Mache A. Experimental analysis of different shaped ribs on heat transfer and fluid flow characteristics. In E3S web of conferences 2020 (pp. 1-4). EDP Sciences.
[33] Dang W, Wang LB. Convective heat transfer enhancement mechanisms in circular tube inserted with a type of twined coil. International Journal of Heat and Mass Transfer. 2021.
[34] Rasool G, Shafiq A, Baleanu D. Consequences of soret–dufour effects, thermal radiation, and binary chemical reaction on darcy forchheimer flow of nanofluids. Symmetry. 2020; 12(9):1-19.
[35] Chanmak P, Krittacom B, Waramit P, Peamsuwan R. Experimental investigation of forced convective heat transfer in circular pipe with wire mesh porous media. In journal of physics: conference series 2021 (pp. 1-9). IOP Publishing.
[36] Fadhil D, Al-turaihi R, Abed A. Effect of semi-circle rib on heat transfer coefficient in a rectangular channel. Frontiers in Heat and Mass Transfer. 2019.
[37] Al KAA, Ibrahim TK, Abdullah MA. Experimental and numerical study of forced convection heat transfer in different internally ribbed tubes configuration using TiO_2 nanofluid. Heat Transfer-Asian Research. 2019; 48(5):1778-804.
[38] Golam AS. Numerical and experimental investigation of heat transfer features in a square duct with internal ribs. WASIT Journal of Engineering Sciences. 2018; 6(3):51-68.
[39] Choi YC, Jeong M, Park YG, Park SH, Ha MY. Direct numerical simulation of flow characteristics and heat transfer enhancement in a rib-dimpled cooling

channel. Journal of Mechanical Science and Technology. 2022; 36(3):1521-35.
[40] Nakhchi ME, Esfahani JA. Numerical investigation of heat transfer enhancement inside heat exchanger tubes fitted with perforated hollow cylinders. International Journal of Thermal Sciences. 2020.
[41] Sadiq HM, Hamza NH. The effect of ribs spacing on heat transfer in rectangular channels under the effect of different types of heat flux in the presence of a nanofluids. Al-Qadisiyah Journal for Engineering Sciences. 2021; 14(2):99-108.
[42] Wang W, Zhang B, Cui L, Zheng H, Klemeš JJ, Wang J. Numerical study on heat transfer and flow characteristics of nanofluids in a circular tube with trapezoid ribs. Open Physics. 2021; 19(1):224-33.
[43] Theeb AH, Mussa MA. Numerical investigation on heat transfer enhancement and turbulent flow characteristics in a high aspect ratio rectangular duct roughened by intersecting ribs with inclined ribs. Journal of Engineering. 2020; 26(5):20-37.
[44] Dhaidan NS, Abbas AK. Turbulent forced convection flow inside inward-outward rib corrugated tubes with different rib-shapes. Heat Transfer-Asian Research. 2018; 47(8):1048-60.
[45] Hashim YA. Heat transfer and fluid flow inside duct with using fan-shape ribs. Journal of Applied Engineering Science. 2021; 19(2):526-32.
[46] Alwan MS, Hadi JM, Jaafer LH, Jalghaf HK. Study the effect of nano fluid on heat transfer in finned pipe with internal v-cut twisted tape. Journal of Mechanical Engineering Research and Developments. 2020; 43(5):161-77.
[47] Alfarawi S, Abdel-moneim SA, Bodalal A. Experimental investigations of heat transfer enhancement from rectangular duct roughened by hybrid ribs. International Journal of Thermal Sciences. 2017; 118:123-38.
[48] Hammoodi KA, Hasan HA, Abed MH, Basem A, Al-tajer AM. Control of heat transfer in circular channels using oblique triangular ribs. Results in Engineering. 2022.
[49] Papulová Z, Gažová A, Šlenker M, Papula J. Performance measurement system: implementation process in SMEs. Sustainability. 2021; 13(9):1-19.
[50] Delort M, Fakra DA, Malet-damour B, Gatina JC. Measuring the uncertainty assessment of an experimental device used to determine the thermo-optico-physical properties of translucent construction materials. Measurement Science and Technology. 2022; 33(5).
[51] Guide AF. Ansys fluent tutorial guide. Ansys INC nd. 2013.
[52] Lienhard IV, John H. A heat transfer textbook. Phlogiston Press; 2005.
[53] Wang Y, Oon CS, Tran MV, An JY. Investigation on heat transfer and pressure drop performance utilizing GNP-based colloidal suspension flow in finned conduit. In IOP conference series: earth and environmental science 2021 (pp. 1-8). IOP Publishing.

Sarmad A. Abdul Hussein is a Lecturer at Department of Mechanical Engineering, College of Engineering, University of Baghdad, Baghdad, Iraq. He has a PhD in Mechanical Engineering/Thermo-Fluids from College of Engineering, University of Baghdad. He has published more than 6 papers in highly reputable journals. His research interests are in the areas of Heat Transfer, Convection, Computational Fluid Dynamics, Engineering Thermodynamics, Solar Radiation, Fluid Mechanics, etc.
Email: sarmad.alsaraf@coeng.uobaghdad.edu.iq

Suhaib J. Shbailat is a Lecturer at Department of Biomedical Engineering, Al-Esraa University College, Baghdad, Iraq. He has a PhD in Mechanical Engineering/Thermo-Fluids from College of Engineering, University of Baghdad. He has published more than 8 papers in highly reputable journals. His research interests are in the areas of Computer-Aided Engineering CAE, Computational Fluid Dynamic CFD, porous media, Solar Energy, Electronic Equipment Cooling, Thermodynamics, Heat Transfer, Fluid Mechanics, Biomedical Engineering. Biomechanics etc.
Email: suhaib@esraa.edu.iq

Appendix I

S. No.	Abbreviation	Description
1	A	Cross section area (m^2)
2	A_s	Surface Area (m^2)
3	C_P	Specific heat at constant pressure (J/kg.K)
4	D_h	Hydraulic Diameter (m)
5	E	Total energy (kJ)
6	g	Gravitational acceleration (m/s^2)
7	G	Production of turbulent kinetic energy
8	h	Heat transfer coefficient ($W/m^2.K$)
9	I	Identity matrix
10	k	Thermal conductivity (W/m.K)
11	Nu	Nusselt numbers
12	p	Pressure (Pa.)
13	Pr	Prandtl number
14	Re	Reynolds number
15	t	Time (s)
16	T	Temperature (°C)
17	v	Air velocity (m/s)
18	i	Inlet
19	ave.	Average
20	m	Mean
21	o	Outlet
22	s	Surface
23	x	Local Distance